European Journal of Medicinal Chemistry 52 (2012) 313–321

Contents lists available at SciVerse ScienceDirect

European Journal of Medicinal Chemistry

journal homepage: http://www.elsevier.com/locate/ejmech

Short communication

Cobalt, nickel, copper and zinc complexes with 1,3-diphenyl-1*H*-pyrazole-4-carboxaldehyde Schiff bases: Antimicrobial, spectroscopic, thermal and fluorescence studies

Kiran Singh [a,*], Yogender Kumar [a], Parvesh Puri [a], Mahender Kumar [a], Chetan Sharma [b]

[a] Department of Chemistry, Kurukshetra University, Kurukshetra, Haryana 136 119, India
[b] Department of Microbiology, Kurukshetra University, Kurukshetra, Haryana 136 119, India

ARTICLE INFO

Article history:
Received 30 September 2011
Received in revised form
22 February 2012
Accepted 27 February 2012
Available online 3 March 2012

Keywords:
1,3-Diphenyl-1*H*-pyrazole-4-carboxaldehyde
Antimicrobial activity
Thermal studies
1,2,4-Triazole
Fluorescence

ABSTRACT

Two new Schiff bases of 1,3-diphenyl-1*H*-pyrazole-4-carboxaldehyde and 4-amino-5-mercapto-3-methyl/H-1,2,4-triazole [HL^{1-2}] and their Cobalt, Nickel, Copper and Zinc complexes have been synthesized and characterized by elemental analyses, spectral (UV–vis, IR, ^{1}H NMR, Fluorescence) studies, thermal techniques and magnetic measurements. A square planar geometry for Cu(II) and octahedral geometry for Co(II), Ni(II) and Zn(II) complexes have been proposed. In order to evaluate the biological activity of Schiff bases and to assess the role of metal ion on biological activity, the pyrazole Schiff bases and their metal complexes have been studied *in vitro* antibacterial against *Staphylococcus aureus*, *Bacillus subtilis*, *Escherichia coli*, *Pseudomonas aeruginosa* and antifungal against *Aspergillus niger*, and *Aspergillus flavus*. In most of the cases higher activity was exhibited upon coordination with metal ions.

1. Introduction

Finding new species, with a wide spectrum of biological activity (antimicrobial, antiviral) and also low cytotoxicity represents a very important aspect in the biochemical research area. This is due the fact that the pathogens agents continuously undergo mutations and also the drugs used to treat the viral disease develop in time a certain resistance to a particular antibiotic [1–3].

Recently, there has been considerable amount of progress in 1,3-diarylpyrazole chemistry because of the recognition of importance of the pyrazole structure in biological processes as antimicrobial [4], anti-inflammatory [5], antitubercular [6], antitumor [7], anti-angiogensis [8], antiparasitic [9], antiviral [10] and also possesses analgesic and anxiolytic activity [11]. 4-Amino-3-mercapto-1,2,4-triazole derivative is an ideal heterocyclic by virtue of its vicinal nucleophiles amino and mercapto groups constitutes a ready-made building block for construction of various organic heterocycles [12]. Nitrogen containing heterocyclic molecules constitutes the largest portion of chemical entities, which are part of many natural products, fine chemicals and biologically active pharmaceuticals vital for enhancing the quality of life [13]. Schiff bases derived from 3-substituted-4-amino-5-mercapto-1,2,4-triazoles show analgesic, antimicrobial, antidepressant and anti-inflammatory activities [14]. When bioorganic molecules or drugs are bound to metal ions, there is drastic change in their biomimetic properties, therapeutic effects and pharmacological properties. Essential metal ions and their complex are found to be antitumor active, catalytic active, antimicrobial and cytotoxic [15–18].

Keeping in view biological and medicinal properties of triazoles, pyrazoles and the potential chemistry of transition metals, we find it vital to join the chemistry of both moieties in search of designing metal based biological active compounds that could aggressively work against resistant bacterial species. For this accomplishment, 1,3-diphenyl-1*H*-pyrazole-4-carboxaldehyde was reacted with 4-amino-5-mercapto-1,2,4-triazole [HL^1] and 4-amino-5-mercapto-3-methyl-1,2,4-triazole [HL^2] to form a new series of biologically active Schiff bases [HL^{1-2}] and their metal complex with Co(II), Ni(II), Cu(II) and Zn(II) ions. The synthesized ligands and their metal complexes were characterized by different techniques like elemental analyses, spectral studies (UV–vis, IR, ^{1}H NMR, Fluorescence), TGA, magnetic and conductance measurements.

* Corresponding author. Tel.: +91 9812137734.
E-mail address: kiransinghkuk@yahoo.co.in (K. Singh).

0223-5234/$ – see front matter © 2012 Elsevier Masson SAS. All rights reserved.
doi:10.1016/j.ejmech.2012.02.053

2. Pharmacology

2.1. Antibacterial activity (in vitro)

All the newly synthesized ligands [HL^{1-2}] and their metal complexes were screened *in vitro* for their antibacterial activity against two Gram-positive (*Staphylococcus aureus* MTCC 96, *Bacillus subtilis* MTCC 121) and two Gram-negative (*Escherichia coli* MTCC 1652, *Pseudomonas aeruginosa* MTCC 741) bacterial strains by agar well diffusion method as reported in our previous paper [19]. DMSO was used as a negative control whereas Ciprofloxacin was used as positive control. All the bacterial cultures were procured from Microbial Type Culture Collection (MTCC), IMTECH, Chandigarh and subcultured on nutrient agar.

2.2. Antifungal activity (in vitro)

All the newly synthesized ligands [HL^{1-2}] and their metal complexes were screened *in vitro* for their antifungal activity against two fungi, *Aspergillus niger* and *Aspergillus flavus*, the ear pathogens isolated from the patients of Kurukshetra [20] and evaluated by poisoned food technique [19]. The molds were grown on Sabouraud dextrose agar (SDA) at 25 °C for 7 days and used as inocula. DMSO was used as the negative control whereas Fluconazole was used as the positive control. The experiments were performed in triplicates. Diameters of fungal colonies were measured and expressed as percent mycelial inhibition.

$$\text{Percent inhibition of mycelial growth} = (d_c - d_t)/d_c \times 100$$

Where d_c average diameter of fungal colony in negative control sets and d_t average diameter fungal colony in experimental sets.

2.3. Determination of minimum inhibitory concentration (MIC)

MIC is the lowest concentration of an antimicrobial compound that will inhibit the visible growth of a microorganism after overnight incubation. MIC of the various compounds against bacterial strains was tested through a modified agar well diffusion method [21]. In this method, a twofold serial dilution of each synthesized compound was prepared by first reconstituting the compound in DMSO followed by dilution in sterile distilled water to achieve a decreasing concentration range 256–0.5 μg mL^{-1}. A 100 μl volume of each dilution was introduced into wells (in triplicate) in the agar plates already seeded with 100 μl of standardized inoculum (10^6 cfu mL^{-1}) of the test microbial strain. All test plates were incubated aerobically at 37 °C for 24 h and observed for the inhibition zones. Ciprofloxacin was used as positive control.

3. Results and discussion

The synthesis of Schiff bases [HL^{1-2}] is schematically represented in Fig. 1. Analytical data indicated the formation of 1:1 and 1:2 metal complexes of HL^{1-2} with Co(II), Ni(II), Cu(II) and Zn(II) metal ions. The molar conductance values of the complexes (measured in 10^{-3} M DMF) are in the range 3.4–8.2 Ω^{-1} cm^2 mol^{-1} indicating the non electrolytic nature [22,23]. The low conductivity values are in agreement with low solubility of metal complexes in water, ethanol, chloroform, acetone and most organic solvents. On the other hand, they are soluble in DMSO, DMF and decomposed at higher temperature. The purity of ligands and their metal complexes has been checked by TLC.

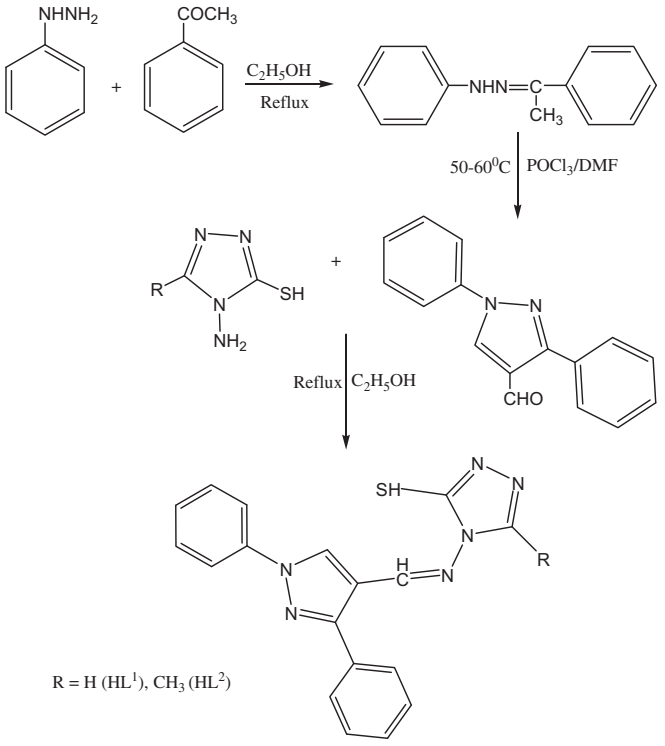

Fig. 1. Scheme for the synthesis of Schiff bases [HL^{1-2}].

3.1. IR spectral studies

The mode of binding of ligands to the metal ions was elucidated by recording the IR spectra of the complexes as compared with the spectra of free ligands (Table 1). The formation of ligands is confirmed by the absence of stretching vibrations due to aldehyde ν(CHO) and amino $\nu(NH_2)$ moiety of triazole and instead, a strong new band appeared at 1615–1618 cm^{-1} corresponding to the azomethine ν(HC=N) group [15,18,19]. After complexation, the band due to azomethine vibration shifted to lower frequency (15–20 cm^{-1}), thus indicating the coordination of the azomethine-N to the metal ion. A characteristic strong band at 2739–2762 cm^{-1} is ascribed to ν(SH), disappeared in the spectra of metal complexes,

Table 1
The important IR frequencies of the ligands and their metal complexes (cm^{-1}).

Compound	ν (N=CH)	ν (C–S)	ν (S–H)	ν ($OOCCH_3$)	ν (H_2O/OH)	ν (M–S)	ν (M–N)
HL^1	1615	–	2739	–	–	–	–
$Co(L^1)(OAc)\cdot 3H_2O$	1597	756	–	1728	3356	352	487
$Co(L^1)_2\cdot 2H_2O$	1598	755	–	–	3350	351	491
$Ni(L^1)(OAc)\cdot 3H_2O$	1592	753	–	1720	3348	348	502
$Ni(L^1)_2\cdot 2H_2O$	1592	753	–	–	3300	350	508
$Cu(L^1)(OAc)\cdot H_2O$	1595	756	–	1726	3318	338	488
$Cu(L^1)_2$	1593	756	–	–	–	340	488
$Zn(L^1)(OAc)\cdot 3H_2O$	1598	750	–	1719	3388	352	503
$Zn(L^1)_2\cdot 2H_2O$	1597	752	–	–	3397	356	511
HL^2	1618	–	2762	–	–	–	–
$Co(L^2)(OAc)\cdot 3H_2O$	1598	756	–	1723	3348	338	499
$Co(L^2)_2\cdot 2H_2O$	1600	758	–	–	3310	342	503
$Ni(L^2)(OAc)\cdot 3H_2O$	1597	764	–	1729	3310	340	495
$Ni(L^2)_2\cdot 2H_2O$	1597	756	–	–	3310	339	509
$Cu(L^2)(OAc)\cdot H_2O$	1593	758	–	1727	3412	353	515
$Cu(L^2)_2$	1595	754	–	–	–	350	520
$Zn(L^2)(OAc)\cdot 3H_2O$	1594	765	–	1730	3388	347	487
$Zn(L^2)_2\cdot 2H_2O$	1597	764	–	–	3387	349	488

confirming deprotonation and coordination of thiol group [24]. This is further supported by the lower frequency band appeared at 750–765 cm^{-1} in the metal complexes due to ν(C–S). The new band in the region of 335–355 and 485–520 cm^{-1} in all metal complexes are assigned to vibrations of ν(M–S) and ν(M–N) bonds, respectively [22,23]. In the spectra of metal complexes a broad band in the region 3300–3415 cm^{-1} indicated the presence of coordinated water molecules. A strong band in the region 1718–1730 cm^{-1} has been assigned to $\nu(OOCCH_3)$ in 1:1 metal complexes [19].

3.2. ^{1}H NMR spectra of Schiff bases and Zn(II) complexes

The ^{1}H NMR spectral data of Schiff bases and Zn(II) complexes have been given in Table 2. Upon comparison with the free ligands, the signal observed at ~14 ppm can be assigned to the –SH protons [22,23]. This signal disappears in the spectra of metal complexes, which confirms the coordination of ligand to metal ion through the deprotonated thiol group. The ligands [HL^{1-2}] showed characteristic azomethine proton signal at δ 9.67 and δ 9.99, respectively (see Supplementary materials). The characteristic signal due to azomethine proton deshielded in the spectra of metal complexes, suggests coordination of azomethine nitrogen atom to metal ion. The aromatic protons present in the ligands (HL^{1-2}) are found as two multiplets at δ 7.42, 7.55 and double doublets at 7.85 and 8.03 ppm, respectively, show a slight shift upon coordination. The triazole-H and pyrazole-H of HL^1 appeared as singlet at δ 8.80 and 9.24 ppm, respectively, and pyrazole-H of HL^2 at 9.29 ppm. In the spectra of 1:1 Zn complexes singlet at δ 1.82 is due to methyl group of acetate ion.

3.3. Magnetic measurements and electronic spectra

The electronic spectra and magnetic moments data of the metal complexes are listed in Table 3. The electronic spectra provided enough information regarding the arrangements of the ligands around the metal ions. The magnetic moments of the Co(II) complexes of HL^{1-2} at room temperature are in the range 4.65–4.75 BM [15]. These values are in good agreement with those reported for octahedral Co(II) complexes. For high spin octahedral complexes of Co(II), two transitions are expected in the electronic spectra; they are $^4T_{1g}(F) \rightarrow {}^4T_{2g}(F)$ (ν_1); $^4T_{1g}(F) \rightarrow {}^4T_{1g}(P)$ (ν_3), ν_2 is not observed, but it can be calculated [25,26] by using relation $\nu_2 = \nu_1 + 10Dq$, which is very close to (ν_3) transition. Also the ratio of second to first transition [26] should lie in the range of 2.1–2.2. Co(II) complexes exhibits two absorption bands in the region 11,240–11,390 cm^{-1} (ν_1) and 21,575–22,225 cm^{-1}(ν_3) and transition energy ratio of second to first is 2.11, corresponding to high spin octahedral complexes. The ligand field parameters (Dq, B, β, β %) have also been calculated (Table 3) for Co(II) complexes by using Band-fitting equation [26]. The Rachah parameter (B) is found to be 764–810 cm^{-1} (<971 cm^{-1}), suggesting an overlapping of ligand metal orbital's. The nephelauxetic ratio (β) for the 1:1 and 1:2 cobalt complexes is less than one suggesting partial covalency in the metal ligand bond.

The electronic spectra of Ni(II) complexes show three absorption band in the region 9999–10,123 cm^{-1}, 16,380–17320 cm^{-1} and 24,885–24,993 cm^{-1}, which were assigned to $^3A_{2g}(F) \rightarrow {}^3T_{2g}(F)$ (ν_1), $^3A_{2g}(F) \rightarrow {}^3T_{1g}(F)$ (ν_2) and $^3A_{2g}(F) \rightarrow {}^3T_{1g}(P)$ (ν_3) transitions [25]. These are the characteristic bands of octahedral environment around Ni(II) ion. The ligand field parameters (Dq, B, β, β%) indicate significant covalent character of the metal ligand bonds. The magnetic moments of the complexes are in the region 3.0–3.5 BM, which agrees with the presence of Ni(II) ion in an octahedral geometry [27].

Cu(II) complexes show absorption band at 18,600–19,020 cm^{-1} are due to the $^2B_{1g} \rightarrow {}^2A_{1g}$ (ν_1) transition. It is a characteristic band of square planar geometry around the Cu(II) [26,28]. The square planar geometry of Cu(II) in the complexes is confirmed by the measured magnetic moment values, 1.73–1.81 BM.

3.4. Fluorescence properties

The fluorescence emission spectra of the Schiff bases HL^{1-2} and their 1:2 metal complexes were recorded in DMF with excitation wavelength 265 nm at room temperature. The fluorescence emission spectrum of HL^1 with its 1:2 metal complexes is depicted in Fig. 2. HL^1 exhibits a strong fluorescence emission at 382 nm, contrast to this partial fluorescence quenching phenomena are observed in its metal complexes with weak fluorescence emission at 393, 400, 367 and 376 nm for Co(II), Ni(II), Cu(II) and Zn(II), respectively. HL^2 shows strong fluorescence band at 376 nm and its Co(II), Ni(II), Cu(II) and Zn(II) complexes exhibit weak emission bands at 402, 390, 380, and 378 nm, respectively. The maximum emission wavelength of Schiff bases is red-shifted about 5–20 nm owing to the formation of complex. It is evident from the fluorescence spectra that, fluorescence emission intensity of Schiff bases decreased dramatically on complex formation with transition metal ions. The decrease in fluorescence intensity with formation of metal complexes is due to decrease in electron density on Schiff bases [15,29]. The decrease in emission maxima were in the order of Zn(II) > Cu(II) > Co(II) > Ni(II).

3.5. Thermal analyses

The thermogravimetric analysis were carried out for $Co(L^1)_2 \cdot 2H_2O$, $Ni(L^1)_2 \cdot 2H_2O$, $Cu(L^2)(OAc) \cdot H_2O$ and $Zn(L^2)(OAc) \cdot 3H_2O$ and are shown in Fig. 3. The decomposition of all the

Table 2
^{1}H NMR spectral data of Schiff bases and Zn(II) metal complexes.

Compound	^{1}H NMR (DMSO-d_6) (ppm)
HL^1 [$C_{18}H_{14}N_6S$]	7.42 (m, 1H, Ar–H), 7.54 (m, 5H, Ar–H), 7.85 (d, 2H, Ar–H), 8.03 (d, 2H, Ar–H), 8.80 (s, 1H, triazole-H), 9.24 (s, 1H, pyrazole-H), 9.67 (s, 1H, –N=CH–), 14.0 (s, 1H, –SH)
$Zn(L^1)(OAc) \cdot 3H_2O$ [$C_{20}H_{22}N_6O_5SZn$]	7.43 (m, 1H, Ar–H), 7.53 (m, 5H, Ar–H), 7.84 (d, 2H, Ar–H), 8.02 (d, 2H, Ar–H), 8.94 (s, 1H, triazole-H), 9.21 (s, 1H, pyrazole-H), 9.99 (s, 1H, –N=CH–), 1.82 (s,3H, C**H**$_3$COO)
$Zn(L^1)_2 \cdot 2H_2O$ [$C_{36}H_{30}N_{12}O_2S_2Zn$]	7.43 (m, 2H, Ar–H), 7.64 (m, 10H, Ar–H), 7.83 (d, 4H, Ar–H), 7.99 (d, 4H, Ar–H), 8.71 (s, 2H, triazole-H), 9.33 (s, 2H, pyrazole-H), 9.99 (s, 2H, –N=CH–)
HL^2 [$C_{19}H_{16}N_6S$]	2.34 (s, 3H, –CH_3), 7.42 (m, 1H, Ar–H), 7.55 (m, 5H, Ar–H), 7.86 (d, 2H, Ar–H), 8.03 (d, 2H, Ar–H), 9.29 (s, 1H, pyrazole-H), 9.99 (s, 1H, –N=CH–), 13.88 (s, 1H, –SH)
$Zn(L^2)(OAc) \cdot 3H_2O$ [$C_{21}H_{24}N_6O_5SZn$]	2.27 (s, 3H, –CH_3), 7.40 (m, 1H, Ar–H), 7.54 (m, 5H, Ar–H), 7.74 (d, 2H, Ar–H), 8.19 (d, 2H, Ar–H), 9.23 (s, 1H, pyrazole-H), 10.12 (s, 1H, –N=CH–), 1.81(s, 3H, C**H**$_3$COO)
$Zn(L^2)_2 \cdot 2H_2O$ [$C_{38}H_{34}N_{12}O_2S_2Zn$]	2.33 (s, 6H, –CH_3), 7.40 (m, 2H, Ar–H), 7.54 (m, 10H, Ar–H), 7.85 (d, 4H, Ar–H), 8.23 (d, 4H, Ar–H), 9.24 (s, 2H, pyrazole-H), 10.14 (s, 2H, –N=CH–)

Table 3
Electronic spectra, magnetic data and ligand field parameters of metal complexes.

Compound	Transitions (cm^{-1})			Dq (cm^{-1})	B (cm^{-1})	ν_2/ν_1	β	β%	μ_{eff} (BM)
	ν_1	ν_2	ν_3						
$Co(L^1)(OAc)\cdot 3H_2O$	11,248	23,767[a]	21,584	1251.9	773.8	2.11	0.796	20.4	4.73
$Co(L^1)_2\cdot 2H_2O$	11,376	24,021[a]	21,578	1264.5	764.7	2.11	0.787	21.3	4.65
$Ni(L^1)(OAc)\cdot 3H_2O$	9980	15,479	23,584	998.0	608.2	1.55	0.584	41.6	3.32
$Ni(L^1)_2\cdot 2H_2O$	9899	15,458	23,680	989.9	629.4	1.56	0.604	39.6	3.29
$Cu(L^1)(OAc)\cdot H_2O$	18,999			–	–	–	–	–	1.78
$Cu(L^1)_2$	19,011			–	–	–	–	–	1.73
$Co(L^2)(OAc)\cdot 3H_2O$	11,389	24,088[a]	22,222	1269.9	809.5	2.11	0.833	16.7	4.82
$Co(L^2)_2\cdot 2H_2O$	11,275	23,848[a]	22,010	1257.3	802.2	2.11	0.826	17.4	4.78
$Ni(L^2)(OAc)\cdot 3H_2O$	9920	15,174	24,883	992.0	686.4	1.52	0.659	34.1	3.11
$Ni(L^2)_2\cdot 2H_2O$	9935	15,230	24,887	988.7	687.4	1.53	0.660	34.0	3.09
$Cu(L^2)(OAc)\cdot H_2O$	18,583			–	–	–	–	–	1.80
$Cu(L^2)_2$	18,610			–	–	–	–	–	1.81

[a] Calculated.

complexes ended with oxide formation [18,19,22,23]. The determined temperature ranges, percentage mass losses, and thermal effects accompanying the changes in the coordination compounds on heating revealed the following finding (Table 4). In case of $Co(L^1)_2\cdot 2H_2O$ complex, the first step 80–200 °C, results in a mass loss of 4.6% (calcd. 4.6%) corresponding to loss of two water molecules. The second step in the temperature range 200–300 °C corresponding to loss of pyrazole moieties with mass loss 57.7% (calcd. 59.0%) and third steps (300–700 °C) correspond to removal of two triazole molecules with mass loss of 26.7% (calcd. 28.7%) of the ligand leaving metal oxide as residue. The thermal decomposition of Ni complex took place in three steps as indicated by TG curve around 80–197, 197–392 and 392–700 °C corresponding to mass loss of water molecules, pyrazole and triazole moieties, respectively. In case of Cu complex decomposition took place in three steps corresponding to loss of coordinated water molecule, organic (acetate group and pyrazole) and triazole moiety around 80–175, 175–305 and 305–700 °C, respectively. The decomposition of Zn complex also takes place in three major stages. The first and second stage is consisting of loss of water molecules and organic (acetate group and pyrazole) moiety in temperature range 80–408 °C. The third step corresponds to decomposition of triazole molecule at 408–700 °C in the TG curve. The results show good agreement with the formulae suggested from the analytical data.

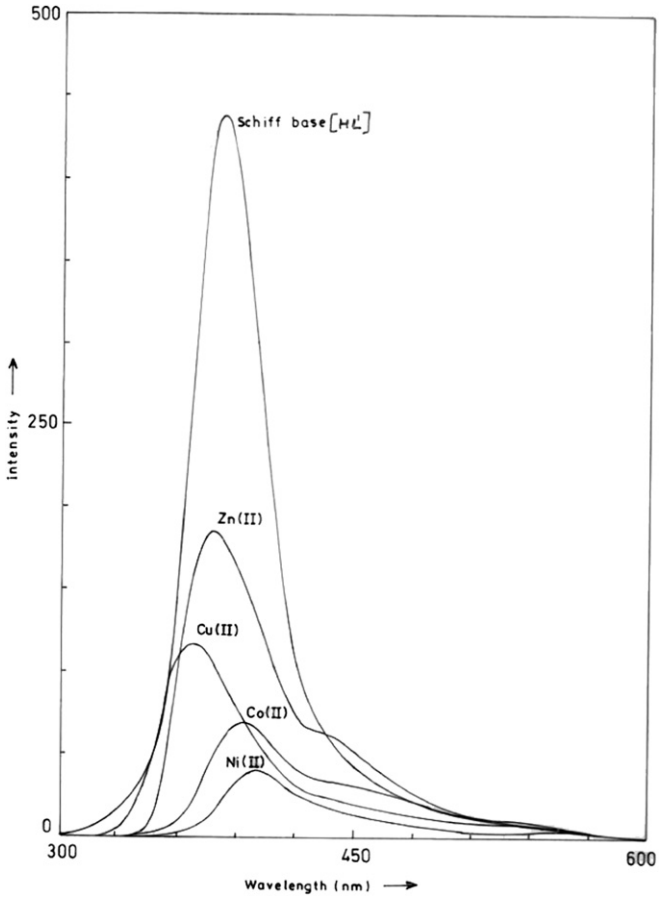

Fig. 2. Fluorescence emission spectra of Schiff base [HL^1] and its metal complexes.

3.5.1. Determination of degradation activation energy

Coats–Redfern equation [30] (equation (1)) is used to evaluate thermal degradation activation energy (E, kJ mol^{-1}) and degradation mechanism for $Co(L^1)_2\cdot 2H_2O$, $Ni(L^1)_2\cdot 2H_2O$, $Cu(L^2)(OAc)\cdot H_2O$ and $Zn(L^2)(OAc)\cdot 3H_2O$.

$$\ln\left[\frac{g(\alpha)}{T^2}\right] = \ln\left[\frac{AR}{E\beta}\right] - \frac{E}{RT} \quad (1)$$

In above equation, β is the heating rate (°C min^{-1}), T is temperature, R is the universal gas constant, A is the pre-exponential factor (min^{-1}), α is the degree of conversion and $g(\alpha)$

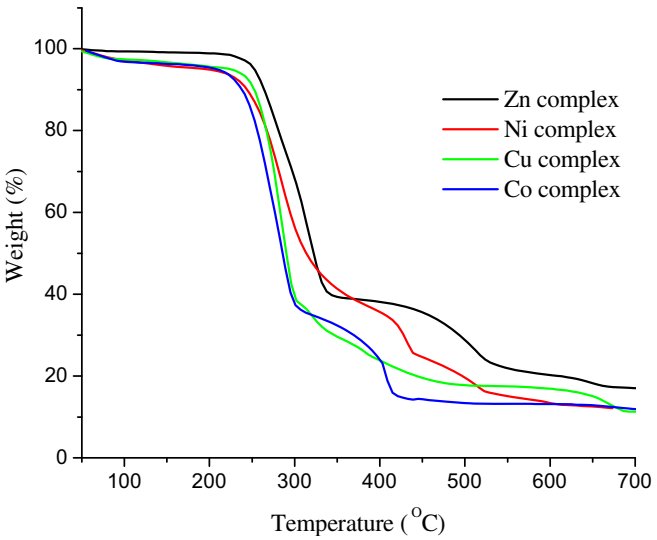

Fig. 3. Thermogravimetric curves of metal complexes.

Table 4
Thermogravimetric characteristics of metal complexes.

Compound	Decomposition stages & assignment	Temp. (°C)	% Weight loss found (calcd.)
$Co(L^1)_2\cdot 2H_2O$	1, Water molecules	80–200	4.6(4.6)
$[C_{36}H_{30}CoN_{12}O_2S_2]$	2, Organic moiety	200–300	57.7(59.0)
	3, Triazole moiety	300–700	26.7(28.7)
$Ni(L^1)_2\cdot 2H_2O$	1, Water molecules	80–197	4.8(4.6)
$[C_{36}H_{30}N_{12}NiO_2S_2]$	2, Organic moiety	197–392	58.4(59.1)
	3, Triazole moiety	392–700	25.8(28.9)
$Cu(L^2)(OAc)\cdot H_2O$	1, Water molecules	80–175	3.5(3.6)
$[C_{21}H_{20}CuN_6O_3S]$	2, –OAc & organic moiety	175–305	58.5(58.2)
	3, Triazole moiety	305–700	22.3(25.4)
$Zn(L^2)OAc\cdot 3H_2O$	1, Water molecules	80–263	10.0(10.1)
$[C_{21}H_{24}N_6O_5SZn]$	2, –OAc, organic moiety	263–408	52.1(54.3)
	3, Triazole moiety	408–700	21.0(23.6)

is degradation mechanism defined by various models as given in Table 5. E can be calculated from the slope of the graph between $\ln[g(\alpha)/T^2]$ and $1/T$. Table 5 presents the activation energy values produced using equations of various models with Coats–Redfern method. To choose the best mechanism among the various models, two conditions are imposed on the results i.e. firstly, models resulting into negative values and secondly, models producing values corresponding to low regression coefficients (r^2) in either degradation stage are summarily neglected. Noticeably, the second order mechanism with $g(\alpha) = (1-\alpha)^{-1} - 1$, results positive E values for the complexes and with best r^2 data among all models producing positive E values (Table 5) and the corresponding plots are shown in Fig. 4. Based on the E_2 (second stage) values as deduced using second order model, following stability order is suggested: Cu > Co > Zn > Ni complex.

3.6. Antimicrobial discussion

The ligands (HL^{1-2}), metal complexes, standard drugs and DMSO solvent were screened separately for their antibacterial activity against Gram-positive (*S. aureus*, *B. subtilis*) and Gram-negative (*E. coli*, *P. aeruginosa*) bacteria and antifungal activity against *A. niger* and *A. flavus*. The microbial results are summarized in Tables 6–8. The antimicrobial studies suggested that the Schiff bases are biologically active and their metal complexes showed significantly enhanced antibacterial and antifungal activity against microbial strains in comparison to the free ligands. Positive controls (Standard drug) produced significantly sized inhibition zones against the tested bacteria and fungi; however, negative control (DMSO) produced no observable inhibitory effect against any of the test organisms.

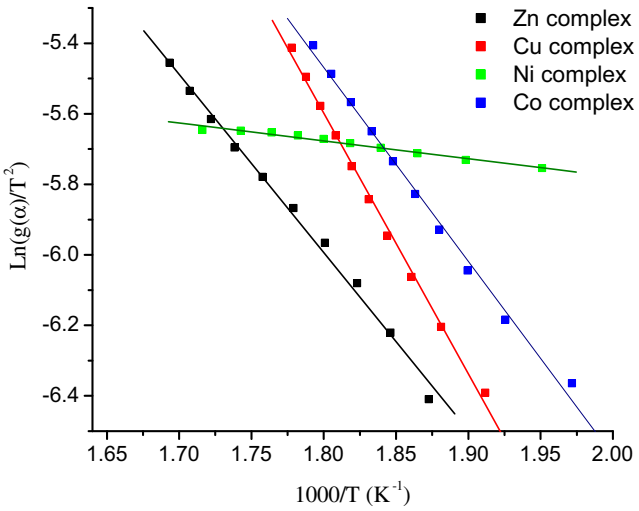

Fig. 4. Coats–Redfern plots for the four compounds using second order mechanism.

Tested compounds showed zone of inhibition ranging 16 mm–28 mm against the Gram-positive bacteria and between 13 mm and 24 mm against Gram-negative bacteria. The ligands (HL^{1-2}) show zone of inhibition ranging 17.6 mm–19.6 mm against Gram-positive bacteria and 13.3 mm–15.6 mm against Gram-negative bacteria. It has been observed that the metal complexes showed increased zone of inhibition against the bacterial strains (Table 6) as compared to ligands ranging 13.0–27.6 mm. On the basis of zone of inhibition produced against the test bacterium, compound **9** was found to be most effective against *S. aureus*, *B. subtilis*, *E. coli* and *P. aeruginosa* with zone of inhibition of 27.6 mm, 25.6 mm, 24.0 mm and 21.0 mm, respectively (Table 6). However, some of the compounds in this series were not effective against any Gram-negative bacteria. The MIC results suggest that the ligands and their complexes (Table 7) showed a moderate activity against the bacterial strains as compared to the standard drug (Ciprofloxacin). In the whole series, the MIC of synthesized compounds ranged 10.0–481.7 μM against Gram-positive bacteria and 19.5–710.2 μM against Gram-negative bacteria. MIC results revealed that the metal complexes are more effective against the antibacterial strains as compared to the Schiff bases. Compound **9** was found to be best antibacterial agent exhibited the lowest MIC 10.0 μM against *S. aureus* and *B. subtilis* (Table 7). The results of our study are in accordance with the reports of earlier workers

Table 5
Activation energy values calculated using Coats–Redfern method.

Model	Cu complex		Ni complex		Zn complex		Co complex	
	$E_2(r^2)$[a]	$E_3(r^2)$[a]	$E_2(r^2)$	$E_3(r^2)$	$E_2(r^2)$	$E_3(r^2)$	$E_2(r^2)$	$E_3(r^2)$
Power law, $\alpha^{1/4}$	17.8(0.993)	−8.2(0.99)	6.7(0.93)	−8.7(0.998)	7.6(0.941)	−9.9(0.998)	10.5(0.975)	−8.7(0.999)
Power law, $\alpha^{1/3}$	26.0(0.995)	−7.4(0.98)	11.9(0.96)	−7.8(0.996)	13.2(0.965)	−9.5(0.997)	17.1(0.984)	−8.25(0.999)
Power law, $\alpha^{1/2}$	44.6(0.96)	−6.1(0.96)	22.5(0.976)	−6.5(0.986)	28.1(0.958)	−8.6(0.99)	30.1(0.988)	−7.2(0.999)
Avrami–Erofeev, $[-\ln(1-\alpha)]^{1/4}$	22.8(0.999)	−5.6(0.97)	9.7(0.978)	−6.0(0.963)	13.0(0.964)	−8.2(0.994)	15.0(0.998)	−6.7(0.994)
Avrami–Erofeev, $[-\ln(1-\alpha)]^{1/3}$	33.3(0.999)	−4.1(0.93)	15.9(0.986)	−4.5(0.88)	20.4(0.974)	−7.5(0.987)	23.3(0.989)	−5.5(0.983)
Avrami–Erofeev, $[-\ln(1-\alpha)]^{1/2}$	54.9(0.999)	−1.1(0.33)	28.6(0.99)	−1.2(0.189)	35.5(0.98)	−5.6(0.948)	39.2(0.997)	−3.2(0.884)
One dimensional diffusion, α^2	205.0(0.997)	6.1(0.71)	117.3(0.97)	7.0(0.797)	140.5(0.973)	−1.1(0.16)	147.4(0.992)	1.9(0.651)
Diffusion control (Janders), $[1-(1-\alpha)^{1/3}]^2$	111.4(0.999)	3.8(0.689)	61.8(0.996)	4.3(0.565)	74.8(0.98)	−2.5(0.62)	80.8(0.997)	0.6(0.105)
Diffusion control (Crank) $1-(2/3)\alpha-(1-\alpha)^{2/3}$	222.6(0.999)	12.9(0.88)	127.7(0.99)	14.3(0.856)	152.7(0.7)	3.16(0.45)	162.4(0.997)	7.4(0.81)
Mampel (first order), $-\ln(1-\alpha)$	118.4(0.999)	8.0(0.87)	66.0(0.993)	8.5(0.718)	74.1(0.994)	0.1(0.001)	87.1(0.998)	3.8(0.694)
Second order, $(1-\alpha)^{-1} - 1$	141.5(0.999)	24.3(0.98)	79.8(0.995)	25.3(0.82)	96.7(0.993)	9.6(0.737)	108.3(0.998)	17.2(0.883)
Contracting cylinder, $1-(1-\alpha)^{1/2}$	107.9(0.99)	2.2(0.42)	59.8(0.98)	2.5(0.387)	72.5(0.978)	−3.6(0.82)	77.8(0.996)	0.8(0.264)
Contracting Sphere, $1-(1-\alpha)^{1/3}$	111.4(0.999)	3.8(0.68)	61.8(0.996)	4.3(0.565)	74.9(0.98)	−2.5(0.65)	80.8(0.997)	0.6(0.105)

[a] 2 & 3 stands for second & third stage, r^2 stands for regression coefficient.

Table 6
Antibacterial activity of chemical compounds through agar well diffusion method.

Sr. No.	Compounds	Diameter of growth of inhibition zone (mm)[a]			
		S. aureus	*B. subtilis*	*E. coli*	*P. aeruginosa*
1	HL^1	17.6	18.3	13.3	14.3
2	$Co(L^1)(OAc)\cdot 3H_2O$	18.3	18.6	–	13.0
3	$Co(L^1)_2\cdot 2H_2O$	17.3	18.3	15.3	–
4	$Ni(L^1)(OAc)\cdot 3H_2O$	21.6	22.6	18.3	16.3
5	$Ni(L^1)_2\cdot 2H_2O$	20.6	19.6	17.6	16.6
6	$Cu(L^1)(OAc)\cdot H_2O$	16.3	17.6	14.3	16.6
7	$Cu(L^1)_2$	17.6	18.3	–	–
8	$Zn(L^1)(OAc)\cdot 3H_2O$	22.6	24.6	19.3	17.6
9	$Zn(L^1)_2\cdot 2H_2O$	27.6	25.6	24.0	21.0
10	HL^2	18.6	19.6	17.3	15.6
11	$Co(L^2)(OAc)\cdot 3H_2O$	16.3	19.3	–	–
12	$Co(L^2)_2\cdot 2H_2O$	22.6	21.6	17.3	16.3
13	$Ni(L^2)(OAc)\cdot 3H_2O$	16.3	19.3	16.6	16.4
14	$Ni(L^2)_2\cdot 2H_2O$	20.0	19.6	17.6	15.6
15	$Cu(L^2)(OAc)\cdot H_2O$	17.3	19.3	14.3	14.3
16	$Cu(L^2)_2$	15.6	17.0	16.2	14.3
17	$Zn(L^2)(OAc)\cdot 3H_2O$	17.3	19.6	13.3	14.3
18	$Zn(L^2)_2\cdot 2H_2O$	17.6	18.3	17.6	17.0
19	Ciprofloxacin	26.6	24.0	25.0	22.0

– No activity.
[a] Values, including diameter of the well (8 mm), are means of three replicates.

Table 8
Antifungal activity of Schiff bases and their metal complexes.

Sr. No.	Compounds	Mycelial growth inhibition (%)	
		A. niger	*A. flavus*
1	HL^1	45.5	42.5
2	$Co(L^1)(OAc)\cdot 3H_2O$	48.8	44.4
3	$Co(L^1)_2\cdot 2H_2O$	50.0	43.3
4	$Ni(L^1)(OAc)\cdot 3H_2O$	55.5	52.5
5	$Ni(L^1)_2\cdot 2H_2O$	48.8	44.4
6	$Cu(L^1)(OAc)\cdot H_2O$	45.5	41.1
7	$Cu(L^1)_2$	51.1	47.7
8	$Zn(L^1)(OAc)\cdot 3H_2O$	58.8	55.5
9	$Zn(L^1)_2\cdot 2H_2O$	60.0	63.3
10	HL^2	57.7	61.1
11	$Co(L^2)(OAc)\cdot 3H_2O$	51.1	52.5
12	$Co(L^2)_2\cdot 2H_2O$	55.5	58.8
13	$Ni(L^2)(OAc)\cdot 3H_2O$	48.8	51.1
14	$Ni(L^2)_2\cdot 2H_2O$	45.5	48.8
15	$Cu(L^2)(OAc)\cdot H_2O$	52.5	50.0
16	$Cu(L^2)_2$	43.3	45.5
17	$Zn(L^2)(OAc)\cdot 3H_2O$	41.1	44.4
18	$Zn(L^2)_2\cdot 2H_2O$	42.5	47.7
19	Fluconazole	81.1	77.7

[17,18,31], which also showed that the antibacterial activity of ligands is greatly enhanced when it is coordinated to metal ions.

Both of the Schiff bases showed activity against fungal species. However, metal complexes of these Schiff bases show enhanced activity as compared to the uncoordinated compounds, especially with *A. niger*. Of the 18 chemical compounds screened for their antifungal activity, three compounds **8**, **9** and **10** showed more than 55% inhibition of mycelial growth against *A. niger* whereas two compounds **9** and **10** showed more than 60% inhibition of mycelial growth against *A. flavus* (Table 8). The overtone's concept [32] and Tweedy's chelation theory [33] can be used to explain the enhanced in antimicrobial activity of the metal complexes. According to the Overtone's concept of cell permeability, the lipid membrane surrounding the cell favors the passage of only lipid-soluble materials; therefore, liposolubility is an important factor which controls the antimicrobial activity. On chelation, polarity of the metal ion is reduced to a greater extent due the overlapping of the ligand orbital and partial sharing of the positive charge of the metal ion with donor groups. Moreover, delocalization of the π-electrons over the whole chelate ring is increased and lipophilicity of the complexes is enhanced. The increased lipophilicity enhances the penetration of the complexes into the lipid membranes and blocks the metal binding sites in the enzymes of microorganisms. These complexes also disturb the respiration process of the cell and thus block the synthesis of proteins, which restricts further growth of the organism. In general, metal complexes are more active than ligands as they may serve as principal cytotoxic species. Thus exhibiting their broad spectrum nature and can be further used in pharmaceutical industry for mankind, as an antimicrobial agent, after testing its toxicity to human beings.

Table 7
Minimum inhibitory concentration (MIC) (μM) of compounds.

Sr. no.	Compound	*Staphylococcus aureus*	*Bacillus subtilis*	*Escherichia coli*	*Pseudomonas aeruginosa*
1	HL^1	184.7	369.5	739.0	369.9
2	$Co(L^1)(OAc)\cdot 3H_2O$	123.6	123.6	–	162.9
3	$Co(L^1)_2\cdot 2H_2O$	81.4	162.8	81.4	–
4	$Ni(L^1)(OAc)\cdot 3H_2O$	61.8	30.9	247.4	494.9
5	$Ni(L^1)_2\cdot 2H_2O$	40.7	162.9	162.9	325.8
6	$Cu(L^1)(OAc)\cdot H_2O$	263.3	131.6	263.3	526.7
7	$Cu(L^1)_2$	84.4	169.6	–	–
8	$Zn(L^1)(OAc)\cdot 3H_2O$	61.0	30.5	244.3	244.3
9	$Zn(L^1)_2\cdot 2H_2O$	10.0	10.0	40.3	80.7
10	HL^2	177.5	88.7	355.1	710.2
11	$Co(L^2)(OAc)\cdot 3H_2O$	481.7	240.8	–	–
12	$Co(L^2)_2\cdot 2H_2O$	39.32	39.32	314.5	78.6
13	$Ni(L^2)(OAc)\cdot 3H_2O$	120.4	120.4	240.9	240.9
14	$Ni(L^2)_2\cdot 2H_2O$	39.3	157.3	157.3	314.6
15	$Cu(L^2)(OAc)\cdot H_2O$	127.9	255.9	511.9	255.9
16	$Cu(L^2)_2$	327.1	163.5	81.7	40.8
17	$Zn(L^2)(OAc)\cdot 3H_2O$	118.9	59.4	118.9	59.4
18	$Zn(L^2)_2\cdot 2H_2O$	156.0	156.0	19.5	39.0
19	Ciprofloxacin	15.1	15.1	15.1	15.1

– Not tested.

4. Conclusions

The synthesized Schiff bases act as bidentate ligands and coordinated to metal ion through nitrogen and sulphur of thiol group. The bonding of ligand to metal ion is confirmed by elemental analyses, spectral studies (UV–vis, IR, ^{1}H NMR, Fluorescence), TGA, magnetic and conductance measurements. The ligand field parameters (Dq, B, β, $\beta\%$) indicated significant covalent character of the metal ligand bonds. The proposed structures of metal complexes are presented in Fig. 5. The antimicrobial studies suggested that the Schiff bases were found to be biologically active and their metal complexes show significantly enhanced antibacterial and antifungal activity against microbial strains in comparison to the free ligands. Thus, exhibiting their broad spectrum nature and can become a new antimicrobial agent, after further biological studies.

5. Experimental protocols

5.1. Materials and methods

All the chemicals used in the present investigation were of Analytical grade and used without further purification. The elemental analyses (C, H, and N) were carried out at SAIF, Punjab University, Chandigarh by using Perkin–Elmer 2400 Elemental Analyzer. The metal contents were determined using standard gravimetric methods; cobalt was estimated as cobalt pyridine thiocyanate, nickel as nickel dimethylglyoximate, copper as cuprous thiocyanate, and zinc as zinc ammonium phosphate [34]. The FT-IR measurements of neat samples were performed on a MB-

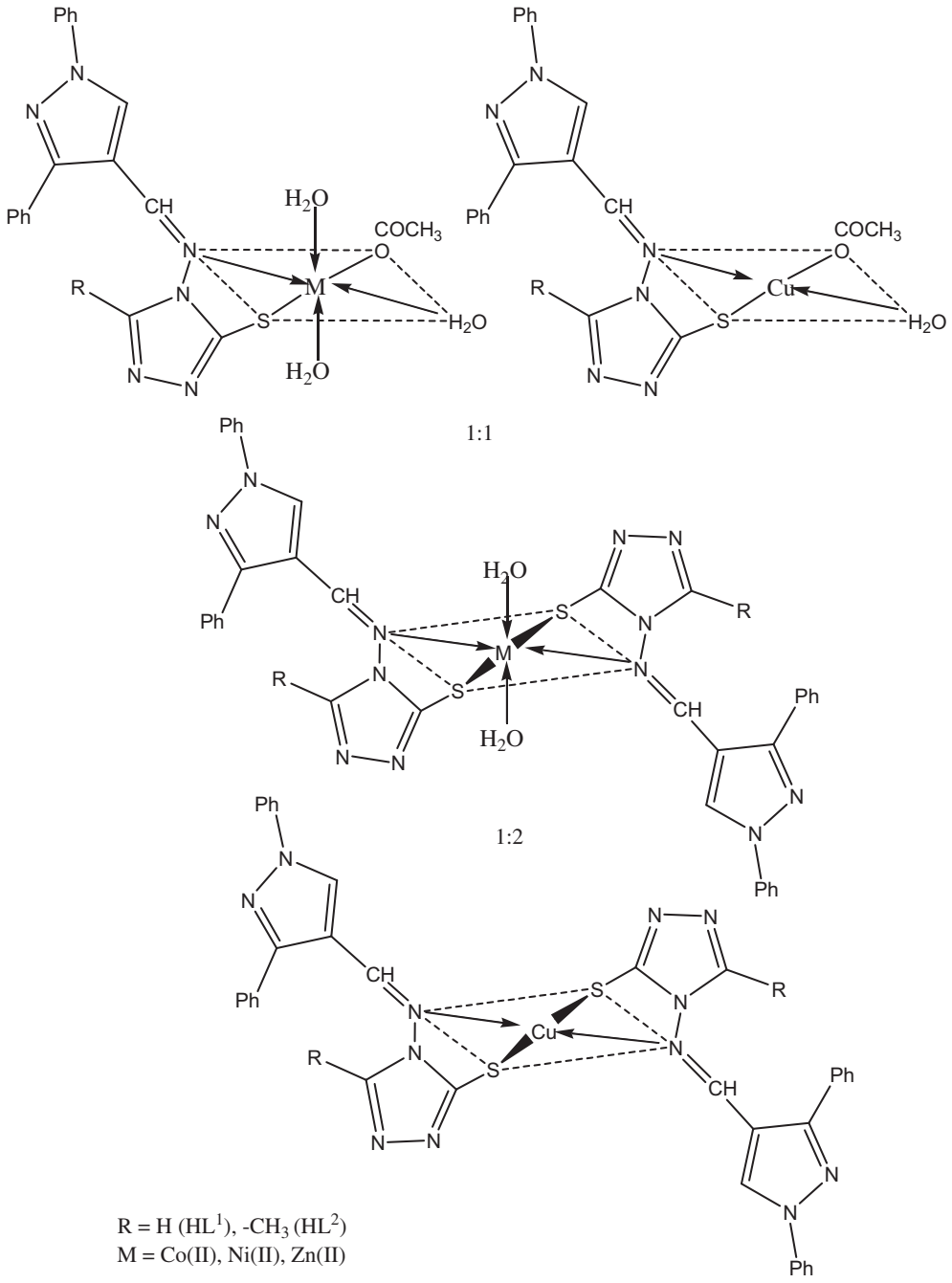

Fig. 5. Proposed structures of metal complexes.

3000 ABB Spectrometer in the range 4000–250 cm^{-1}. The UV–visible absorption spectra of solid complexes were recorded on T 90 (PG Instruments ltd) UV/vis spectrometer in the region 1100–200 nm. Proton NMR spectra were recorded in DMSO-d_6 on a Bruker ACF 300 spectrometer at 300 MH_Z using "tetramethyl silane" as the internal standard. Magnetic moments were measured at Institute Instrumentation Centre, IIT Roorkee on vibrating sample magnetometer (Model 155). The Perkin–Elmer (Pyris Diamond) instrument was used to carry out thermal analysis of metal complexes in atmospheric air (80–700 °C) at a heating rate of 10 °C min^{-1} using a reference to alumina powder. The Perfit electrical melting point apparatus is used to record melting points of the synthesized complexes and are uncorrected. The fluorescence studies of Schiff bases and their metal complexes were recorded on SHIMADZU RF-5301PC spectrophotometer. The solutions of 10^{-3} M concentration were prepared in HPLC grade DMF and the experiment was carried out at room temperature.

5.2. Syntheses

4-Amino-5-mercapto-1,2,4-triazole [35], 4-amino-5-mercapto-3-methyl-1,2,4-triazole [35] and 1,3-diphenyl-1*H*-pyrazole-4-carboxaldehyde [36] were prepared by reported literature method.

5.2.1. 4-[(1,3-Diphenyl-1H-pyrazol-4-ylmethylene)-amino]-5-mercapto-1,2,4-triazole [HL^1]

To a hot ethanolic (20 mL) solution of 4-amino-5-mercapto-1,2,4-triazole (1.08 g, 9.28 mmol), 1,3-diphenyl-1*H*-pyrazole-4-

carboxaldehyde (2.30 g, 9.28 mmol) in ethanol (20 mL) was added with constant stirring and refluxed for 6 h after cooling the mixture to room temperature, the precipitated product thus formed was filtered off, washed with ice cooled ethanol and recrystallized from same solvent. Finally the product dried under vacuum.

Dull white. Yield (60%); m.p. 258–260 °C; Anal. calcd. for $C_{18}H_{14}N_6S$: C, 62.41; H, 4.07; N, 24.26; found: C, 62.38; H, 4.07; N, 24.11%.

5.2.2. 4-[(1,3-Diphenyl-1H-pyrazol-4-ylmethylene)-amino]-5-mercapto-3-methyl-4H-1,2,4-triazole [HL^2]

A solution of 4-amino-5-mercapto-3-methyl-1,2,4-triazole (1.2 g, 9.23 mmol) in ethanol (40 mL) was treated with 1,3-diphenyl-1*H*-pyrazole-4-carboxaldehyde (2.28 g, 9.23 mmol). The reaction mixture was refluxed for 5 h and the solid crude was filtered off and washed with cold ethanol, dried and recrystallized from the same solvent.

Creamish white. Yield (68%); m.p. 227–230 °C; Anal. calcd. for $C_{19}H_{16}N_6S$: C, 63.31; H, 4.47; N, 23.32; found: C, 63.24; H, 4.32; N, 23.31%.

5.2.3. Metal complexes of HL^1 (1:1)

The solid complexes were prepared by mixing hot ethanolic solutions of the HL^1 (0.35 g, 1.03 mmol) with aqueous ethanolic solutions of acetates of Co(II) (0.26 g, 1.03 mmol), Ni(II) (0.26 g, 1.03 mmol), Cu(II) (0.21 g, 1.03 mmol) and Zn(II) (0.23 g, 1.03 mmol), which resulted in the immediate precipitation of metal complexes. The solid complexes were filtered off, washed thoroughly with warm water, with aqueous ethanol to remove unreacted metal acetates or ligands and finally with acetone and vacuo dried.

$Co(L^1)OAc\cdot 3H_2O$: Anal. calcd. for $C_{20}H_{22}CoN_6O_5S$: C, 46.42; H, 4.29; N, 16.24; Co, 11.39; found: C, 46.42; H, 4.22; N, 16.23; Co, 11.36%.

$Ni(L^1)OAc\cdot 3H_2O$: Anal. calcd. for $C_{20}H_{22}N_6NiO_5S$: C, 46.45; H, 4.29; N, 16.25; Ni, 11.35; found: C, 46.43; H, 4.23; N, 16.21; Ni, 11.31%.

$Cu(L^1)OAc\cdot H_2O$: Anal. calcd. for $C_{20}H_{18}CuN_6O_3S$: C, 49.43; H, 3.73; N, 17.29; Cu, 13.08; found: C, 49.40; H, 3.71; N, 17.28; Cu, 13.00%.

$Zn(L^1)OAc\cdot 3H_2O$: Anal. calcd. for $C_{20}H_{22}N_6O_5SZn$: C, 45.85; H, 4.23; N, 16.04; Zn, 12.48; found: C, 45.82; H, 4.18; N, 16.00; Zn, 12.43%.

5.2.4. Metal complexes of HL^1 (1:2)

The aqueous ethanolic solutions of acetates of Co(II) (0.12 g, 0.50 mmol), Ni(II) (0.13 g, 0.50 mmol), Cu(II) (0.10 g, 0.50 mmol) and Zn(II) (0.10 g, 0.50 mmol) were treated with the hot ethanolic solutions of the HL^1 (0.35 g, 1.00 mmol). The products formed were filtered and purified by washing thoroughly with warm water, with aqueous ethanol to remove unreacted metal acetates or ligands and finally with acetone and dried.

$Co(L^1)_2\cdot 2H_2O$: Anal. calcd. for $C_{36}H_{30}CoN_{12}O_2S_2$: C, 55.03; H, 3.85; N, 21.39; Co, 7.50; found: C, 55.00; H, 3.84; N, 21.33; Co, 7.45%.

$Ni(L^1)_2\cdot 2H_2O$: Anal. calcd. for $C_{36}H_{30}N_{12}NiO_2S_2$: C, 55.04; H, 3.85; N, 21.40; Ni, 7.47; found: C, 55.00; H, 3.82; N, 21.40; Ni, 7.22%.

$Cu(L^1)_2$: Anal. calcd. for $C_{36}H_{26}CuN_{12}S_2$: C, 57.32; H, 3.47; N, 22.48; Cu, 8.42; found: C, 57.30; H, 3.41; N, 22.20; Cu, 8.38%.

$Zn(L^1)_2\cdot 2H_2O$: Anal. calcd. for $C_{36}H_{30}N_{12}O_2S_2Zn$: C, 54.58; H, 3.82; N, 21.22; Zn, 8.25; found: C, 54.55; H, 3.75; N, 21.18; Zn, 8.20%.

5.2.5. Metal complexes of HL^2 (1:1)

The solid complexes were prepared by mixing hot ethanolic solutions of the HL^2 (0.36 g, 1.01 mmol) with aqueous ethanolic solutions of acetates of Co(II) (0.25 g, 1.01 mmol), Ni(II) (0.25 g, 1.01 mmol), Cu(II) (0.20 g, 1.01 mmol) and Zn(II) (0.22 g, 1.01 mmol), which resulted in the immediate precipitation of metal complexes. The solid complexes were filtered off, washed thoroughly with warm water, with aqueous ethanol to remove unreacted metal acetates or ligands and finally with acetone and vacuo dried.

$Co(L^2)OAc\cdot 3H_2O$: Anal. calcd. for $C_{21}H_{24}CoN_6O_5S$: C, 47.46; H, 4.55; N, 15.21; Co, 11.09; found: C, 47.42; H, 4.38; N, 15.20; Co, 11.00%.

$Ni(L^2)OAc\cdot 3H_2O$: Anal. calcd. for $C_{21}H_{24}N_6NiO_5S$: C, 47.48; H, 4.55; N, 15.82; Ni, 11.05; found: C, 47.43; H, 4.48; N, 15.21; Ni, 10.98%.

$Cu(L^2)OAc\cdot H_2O$: Anal. calcd. for $C_{21}H_{20}CuN_6O_3S$: C, 50.44; H, 4.03; N, 16.81; Cu, 12.71; found: C, 50.40; H, 4.01; N, 16.38; Cu, 12.38%.

$Zn(L^2)OAc\cdot 3H_2O$: Anal. calcd. for $C_{21}H_{24}N_6O_5SZn$: C, 46.89; H, 4.50; N, 15.62; Zn, 12.16; found: C, 46.74; H, 4.50; N, 15.61; Zn, 12.16%.

5.2.6. Metal complexes of HL^2 (1:2)

The aqueous ethanolic solutions of acetates of Co(II) (0.15 g, 0.60 mmol), Ni(II) (0.15 g, 0.60 mmol), Cu(II) (0.12 g, 0.60 mmol) and Zn(II) (0.13 g, 0.60 mmol) were treated with the hot ethanolic solutions of the HL^2 (0.43 g, 1.20 mmol). The products formed were filtered and purified by washing thoroughly with warm water, with aqueous ethanol to remove unreacted metal acetates or ligands and finally with acetone and dried.

$Co(L^2)_2\cdot 2H_2O$: Anal. calcd. for $C_{38}H_{34}CoN_{12}O_2S_2$: C, 56.08; H, 4.21; N, 20.65; Co, 7.24; found: C, 56.03; H, 4.20; N, 20.63; Co, 7.23%.

$Ni(L^2)_2\cdot 2H_2O$: Anal. calcd. for $C_{38}H_{34}N_{12}NiO_2S_2$: C, 56.10; H, 4.21; N, 20.66; Ni, 7.21; found: C, 55.00; H, 3.82; N, 21.40; Ni, 7.22%.

$Cu(L^2)_2$: Anal. calcd. for $C_{38}H_{30}CuN_{12}S_2$: C, 58.33; H, 3.86; N, 21.48; Cu, 8.12; found: C, 58.33; H, 3.85; N, 21.46; Cu, 8.12%.

$Zn(L^2)_2\cdot 2H_2O$: Anal. calcd. for $C_{38}H_{34}N_{12}O_2S_2Zn$: C, 55.64; H, 4.18; N, 20.49; Zn, 7.97; found: C, 55.63; H, 4.15; N, 20.46; Zn, 7.96%.

Acknowledgements

Yogender Kumar is highly thankful to University Grant Commission, New Delhi for providing Senior Research Fellowship (SRF) and Department of Chemistry, Kurukshetra University Kurukshetra, for providing facilities to carry out this research work.

Appendix A. Supplementary material

Supplementary material associated with this article can be found, in the online version, at doi:10.1016/j.ejmech.2012.02.053.

References

[1] N. J. Thumar, M. P. Patel, Med. Chem. Res. doi 10.1007/s00044-011-9693-2.
[2] J. Peto, Nature 411 (2001) 390–395.
[3] I. Chopra, C. Schofield, M. Everett, A. O'Neill, K. Miller, M. Wilcox, J.M. Fre`re, M. Dawson, L. Czaplewski, U. Urleb, P. Courvalin, Lancet Infect. Dis. 8 (2008) 133–139.
[4] I. Damljanovic, M. Vukicevic, N. Radulovic, R. Palic, E. Ellmerer, Z. Ratkovic, M.D. Joksovic, R.D. Vukicevic, Bioorg. Med. Chem. Lett. 19 (2009) 1093–1096.
[5] A.A. Bekhit, H.M.A. Ashour, Y.S.A. Ghany, A.E.A. Bekhit, A.M. Baraka, Eur. J. Med. Chem. 43 (2008) 456–463.
[6] P.T. Chovatia, J.D. Akabari, P.K. Kachhadia, P.D. Zalawadia, H.S. Joshi, J. Serb. Chem. Soc. 71 (2007) 713–720.
[7] M.D. Joksovic, V. Markovic, Z.D. Juranic, T. Stanojkovic, L.S. Jovanovic, I.S. Damljanovic, K.M. Szecsenyi, N. Todorovic, S. Trifunovic, R.D. Vukicevic, J. Organomet. Chem. 694 (2009) 3935–3942.
[8] A.H. Abadi, A.A.H. Eissa, G.S. Hassan, Chem. Pharm. Bull. 51 (2003) 838–844.
[9] P. Rathelot, N. Azas, H. El-Kashef, F. Delmas, C.D. Giorgio, P. Timon-David, J. Maldonado, P. Vanelle, Eur. J. Med. Chem. 37 (2002) 671–679.
[10] A.I. Hashem, A.S.A. Youssef, K.A. Kandeel, W.S.I. Abou-Elmagd, Eur. J. Med. Chem. 42 (2007) 934–939.
[11] S.C. Shetty, V.C. Bhagat, Asian J. Chem. 20 (2008) 5037–5045.
[12] X. Collin, A. Sauleau, J. Coulon, Bioorg. Med. Chem. Lett. 13 (2003) 2601–2605.
[13] B. Kalluraya, B. Lingappa, N.S. Rai, Phosphorus, Sulfur Silicon Relat. Elem. 182 (2007) 1393–1401.
[14] O. Bekircan, H. Bektas, Molecules 11 (2006) 469–477.

[15] S.A. Patil, S.N. Unki, A.D. Kulkarni, V.H. Naik, P.S. Badami, Spectrochim. Acta Part A 79 (2011) 1128–1136.
[16] H.A. El-Boraeya, R.M. Abdel-Rahmanb, E.M. Atia, K.H. Hilmy, Cent. Eur. J. Chem. 8 (2010) 820–833.
[17] Z.H. Chohan, S.H. Sumrra, M.H. Youssoufi, T.B. Hadda, Eur. J. Med. Chem. 45 (2010) 2739–2747.
[18] K. Singh, M.S. Barwa, P. Tyagi, Eur. J. Med. Chem. 41 (2006) 147–153.
[19] K. Singh, Y. Kumar, P. Puri, C. Sharma, K.R. Aneja, Med. Chem. Res. (2011). doi:10.1007/s00044-011-9683-4.
[20] K.R. Aneja, C. Sharma, R. Joshi, Inter. J. Otorhinolaryngol. 74 (2010) 604–607.
[21] M.I. Okeke, C.U. Iroegbu, E.N. Eze, A.S. Okoli, C.O. Esimone, J. Ethnopharmacol. 78 (2001) 119–127.
[22] K. Singh, D.P. Singh, M.S. Barwa, P. Tyagi, Y. Mirza, J. Enz. Inhib. Med. Chem. 21 (2006) 557–562.
[23] K. Singh, D.P. Singh, M.S. Barwa, P. Tyagi, Y. Mirza, J. Enz. Inhib. Med. Chem. 21 (2006) 749–755.
[24] A.D. Kulkarni, S.A. Patil, V.H. Naik, P.S Badami, Med. Chem. Res. 20 (2011) 346–354.
[25] F.A. Cotton, G. Williknson, C.A. Murillo, M. Bochman, Advanced Inorganic Chemistry, sixth ed. Wiley, New York, 2003.
[26] A.B.P. Lever, Inorganic Spectroscopy, Elsvier, Amsterdam, 1968.
[27] K.A. Mehla, J. Enz. Inhib. Med. Chem. 23 (2008) 285–295.
[28] A.H. Osman, M.S. Saleh, M.M. Sanaa, Synth. React. Inorg. Met.-Org. Chem. 34 (2004) 1069–1085.
[29] Q.H. Wang, W. Weng, J.M. Liu, L.Z. Cai, G.C. Guo, J. Coord. Chem. 59 (2006) 485–492.
[30] A.W. Coats, J.P. Redfern, Nature 201 (1964) 68–69.
[31] V.P. Singh, A. Katiyar, S. Singh, Biometals 21 (2008) 491–501.
[32] N. Raman, A. Kulandaisamy, K. Jayasubramanian, Polish J. Chem. 76 (2002) 1085–1094.
[33] B.G. Tweedy, Phytopathology 55 (1964) 910.
[34] A.I. Vogel, Text Book of Quantitative Chemical Analysis Longmans, Addison Wesley, London, 1999.
[35] S. Bala, R.P. Gupta, M.L. Sachdeva, A. Singh, H.K. Pujari, Indian J. Chem. Sect. B. 16 (1978) 481–483.
[36] A.Q. Ather, M.N. Tahir, M.A. Khan, K. Mehmood, F. Chaudhary, Acta Cryst. E66 (2010) 3170.